JOURNAL OF MASS SPECTROMETRY, VOL. 31, 339–350 (1996)

SPECIAL FEATURE: PERSPECTIVE

Surface-induced Dissociation: An Effective Tool to Probe Structure, Energetics and Fragmentation Mechanisms of Protonated Peptides

Ashok R. Dongré,† Árpád Somogyi†‡ and Vicki H. Wysocki†§
Department of Chemistry, Virginia Commonwealth University, Richmond, Virginia 23284-2006, USA

The utility of surface-induced dissociation (SID) to probe the structure, energetics and fragmentation mechanisms of protonated peptides is discussed and demonstrated. High internal energy deposition provided by low-energy (eV range) ion–surface collisions yields extensive fragmentation of protonated peptides, allowing relatively uncomplicated and rapid sequence analysis of oligopeptides. SID of multiply protonated peptides is illustrated for peptides with molecular mass of up to ~5000 u. It is also illustrated that SID combined with electrospray ionization (ESI) provides a distinctive experimental technique to determine the energetics and mechanisms of peptide fragmentation. The relative position of ESI/SID fragmentation efficiency curves (plots of percentage fragmentation *vs.* laboratory collision energy) for peptides can be utilized to estimate relative energetics of peptide fragmentation and even to predict proton localization sites. The observed trends support the essential role of the mobile proton model in understanding peptide fragmentation by low-energy tandem mass spectrometry.

KEYWORDS: surface-induced dissociation; protonated peptides; structure; energetics; fragmentation mechanisms

INTRODUCTION

Tandem mass spectrometry (MS/MS) is a well established analytical technique for the characterization of structures of molecules and for investigations of gas-phase ion chemistry.[1,2] Activation of selected ions by collisions with gaseous targets, termed collision-induced dissociation (CID) or collision-activated dissociation (CAD), is the most widely used activation method for ion structure determination by MS/MS. This paper describes results obtained for protonated peptides by an alternative activation technique, surface-induced dissociation (SID).[3–5] One of the motivations for the development of SID as an activation method was the realization of certain limitations of gas-phase collisional activation. Gas-phase collisional activation (CID) does not always provide enough internal energy deposition to fragment large ions, in particular biomolecules, which are a current focus of research in mass spectrometry. On the other hand, it has been demonstrated that with SID a significant portion of the incident ion kinetic energy is converted into internal energy,[5–15] suggesting that SID may prove to be a more effective activation method for the fragmentation of large ions. This expectation is borne out by the fragmentation spectra of multiply charged peptides shown later in this paper.

The SID experiment is simple: mass-selected ions are made to collide with a surface and the products scattered from the surface are mass analyzed. Cooks and co-workers[5–9] demonstrated that low energy (10–200 eV) collisions of ions with surfaces can lead to extensive and structurally informative fragmentation, and that the degree of fragmentation can be easily controlled by varying the laboratory collision energy of the incident ions. An important feature of SID is that the percentage of kinetic energy (T) converted to internal energy (V) is comparatively high, regardless of the surface considered. $T \rightarrow V$ conversions have been reported to be in the range of 12–35% for a variety of different projectiles (e.g. small organics, metal carbonyls, and alkali metal halide clusters) colliding with a variety of surface types.[5–15] Higher energy conversion is consistently observed for silicon surfaces or fluorocarbon-coated surfaces than for graphite surfaces or hydrocarbon-coated surfaces. The energy conversion and relative contribution of different ion–surface collision processes (e.g. dissociation, reaction, neutralization and chemical sputtering; see below) depend on the impact angle(s) between the ion beam and surface, with less effective $T \rightarrow V$ conversions for more glancing collisions. In addition to high average internal energy deposition, SID also offers deposition of a narrow distribution of internal energy which can be easily shifted to higher or lower

† Present address: Department of Chemistry, University of Arizona, Tucson, AZ 85721, USA.
§ Author to whom correspondence should be addressed.
‡ On leave from the Central Research Institute for Chemistry of the Hungarian Academy of Sciences, P.O. Box 17, H-1525, Budapest, Hungary.

CCC 1076–5174/96/040339–12

Received 10 January 1996
Accepted 23 January 1996

average internal energy with variation of the collision energy.[5–15]

A variety of different processes occur when a mass-selected ion collides with a surface (see Fig. 1).[5,16] However, the relative contribution of these different processes occurring at the surface depends on surface type, the incident angle and the projectile ions investigated. For ion structure determination, the major process of interest involves inelastic collisions of polyatomic ions with a surface, leading to dissociation of the impinging ions (SID). Other important processes are reactive collisions of ions, including addition of surface constituents to selected projectiles, and charge exchange reactions. Ion–surface reactions have been the subject of numerous publications and this area has recently been reviewed.[16] The reactions that occur at the surface are specific to the adsorbed surface material and the projectile ion and, in certain cases, are observed in fairly high yields. These reactions have the potential to be used for surface characterization or surface etching. In general, large even-electron projectile ions such as protonated peptides do not undergo significant ion–surface reactions (see spectra below).

Neutralization of the projectile ion upon collision with the surface by charge exchange is a troublesome ion–surface reaction if projectile ion characterization is desired. Neutralization of the ions leads to charge transfer to the surface and can also lead to subsequent release of surface-adsorbed species, in a process called chemical sputtering (an additional method for surface analysis). In an attempt to reduce neutralization at the surface and obtain a well characterized, reproducible surface, Cooks and co-workers[5,7–9,16] and Wysocki and co-workers[14,17–19] have employed self-assembled monolayer (SAM) coatings, chemically bound to metal surfaces, as target surfaces for SID studies. In addition to self-assembled monolayer films bound to metal surfaces, a variety of surface types have also been successfully used for SID. Metals[5,20] such as stainless steel and brass with adventitious hydrocarbon adsorbates and even semiconductor materials[12] such as silicon and graphite have proved to be successful targets for the dissociation of polyatomic ions at surfaces. Recently, a thin coating of liquid fluorocarbon polymer film (with very low vapor pressure) on a metal substrate has been successfully used to perform SID.[9] Several of these different types of surfaces were investigated to improve charge retention, i.e. reduce neutralization. The percentage of the incident ion beam that survives surface collision, i.e., does not undergo neutralization at the surface, is defined as the total scattered ion efficiency (%E). The total scattered ion efficiency of the surface is usually calculated by measuring the ratio of ion current obtained by operating the instrument in the *transmission mode* (deflection of the mass-selected ion beam without collision with the surface) and in the *SID mode* (the mass-selected ion beam is made to collide with the surface, and the total ion current is measured), while keeping the detector voltage constant.[5,17] This method has the advantage of correcting for inefficiencies in transmission through the mass analyzers. In using this method to evaluate surface efficiency, it is assumed that all sources of ion loss are equal in both the transmission and SID mode. In this laboratory, efficiency values measured by a different method gave similar values; these values were obtained by comparing the current measured at a chemically modified surface with that measured at a bare metal surface.[15] Measured efficiency values vary over a wide range from 1% to 65% and depend on the type of surface and also the nature of the incident projectile ion.[5,13,15–17] For example, fluorocarbon surfaces yield very high efficiencies (~60%) because their high ionization energies (*IE*), compared with the *IE* of common organic analytes, minimize neutralization.[5,15–17]

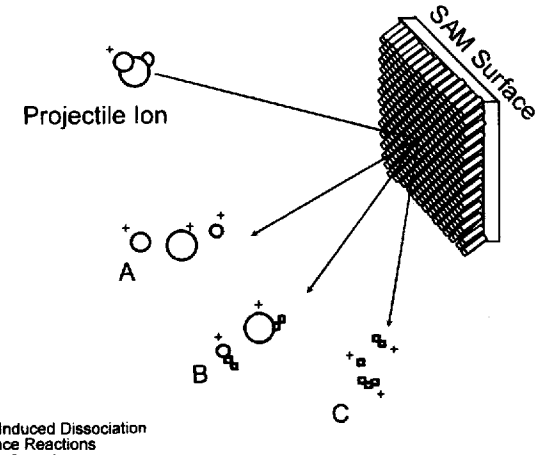

Figure 1. Schematics of different processes occurring during low-energy ion–surface collisions: (A) fragmentation of the selected projectile ion; (B) ion–surface reactions between the projectile ion and the surface material (monolayer or physisorbed material); (C) chemical sputtering of the surface material as a result of charge exchange processes.

INSTRUMENTATION

Surface-induced dissociation was demonstrated in the mid-1970s using high-energy ion beams where collisions with walls led to ion dissociation in double-focusing sector instruments.[3a] In the mid-1980s, a hybrid instrument was designed specifically to perform SID. This hybrid instrument (BQ)[3–5] consisted of a magnetic sector to select the ion of interest, a set of decelerating lenses to control the collision energy with the surface and a quadrupole mass analyzer to collect the products scattered from the surface. In addition to hybrid instruments, four-sector instruments,[21] tandem quadrupole instruments,[22,23] a sector time-of-flight (TOF) instrument,[24] tandem time-of-flight (TOF/TOF) instruments,[25,26] Fourier transform ion cyclotron resonance (FTMS) instruments[27–29] and quadrupole ion trap instruments[30] have been successfully employed to accomplish SID. Deceleration lens assemblies are necessary in sector instruments to achieve low-energy collisions with the surface. SID in FTMS and quadrupole ion trap instruments is performed by trapping the ions and then accelerating them into the walls of the trap, or onto a probe placed at one end of the FTMS cell. This results in dissociation of the mass-selected ion and allows subsequent analysis of the dissociation products. Ion–surface collisions have been accomplished in a

reflectron TOF instrument by placing the surface at the end of the reflector.[12]

The majority of SID experiments performed to date have been performed with non-linear instrument geometries (i.e. MS1–MS2 analyzer angles placed from 70° to 120°). In contrast, commercially available tandem mass spectrometers, both sector and quadrupole instruments, are designed for the more conventional gas-phase CID experiments and the analyzers are thus arranged linearly. In order to provide a simple means to adapt existing mass spectrometers to perform SID, various in-line ion–surface collision cells have been designed and characterized, and microchannel plates have also been tested as possible in-line collision devices.[24,31] In both tandem sector instruments and tandem quadrupole mass spectrometers, the ion beam is deflected from its normal path by an electric field and made to collide with the surface and the product ions are then extracted back onto the normal path and analyzed.

EXPERIMENTAL

The results presented in this paper were obtained on a tandem mass spectrometer specifically designed for low-energy ion–surface collisions (Fig. 2).[23] The instrument consists of two 4000 u quadrupoles (Extrel, Pittsburgh, PA, USA) arranged in a 90° geometry with the surface positioned at the intersection of the ion optical paths of both the quadrupoles. The angle between the incident ion beam and the surface normal is typically kept between 45° and 50°. Emergent angles are not known, but the ion optical system is designed to collect ions over a wide range of angles. The surfaces are mounted on a ceramic plate which is designed to hold multiple surfaces (see Fig. 2). This is advantageous as a variety of different surface types can be analyzed and/or used for analysis of a specific analyte under the same experimental conditions.[17] Different surfaces can be brought into the incident ion beam path simply by moving the surface holder perpendicular to the plane of the quadruples (see Fig. 2). A typical ion–surface collision experiment is carried out by selecting an ion of interest with the first quadrupole, causing it to collide with the surface, collecting the scattered product ions with a series of focusing lenses and performing the final mass analysis with the second quadrupole. The laboratory collision energy is determined by the potential difference between the ion source and the surface or, for multiply charged ions, by the product of potential difference and the charge state selected.

As mentioned in the Introduction, judicious choice of surface characteristics is essential to perform SID efficiently. The chemical composition of the surface plays an important role in the studies of ion–surface collisions. Traditionally, surface science investigations are performed at well characterized metal surfaces using ultra-high vacuum conditions [$>10^{-9}$ Torr (1 Torr = 133.3 Pa)]. However, ion–surface collision experiments can also be performed under more modest vacuum conditions more readily compatible with high-pressure sources (e.g. for experiments performed in our laboratory the manifold pressures are in the range 10^{-5}–10^{-7} Torr). Self-assembled monolayer surfaces have proved to be excellent substrates for investigation of SID and/or other ion–surface collision processes under these conditions. Chemically modified self-assembled monolayer surfaces (illustrated schematically in Fig. 1) are easily prepared by using gold surfaces (1000 Å of vapor deposited gold on a chromium overlayer on silica obtained from Evaporated Metal Films, Ithaca, NY, USA) by immersing the gold in 1 mM, alkene thiol solution in ethanol for 24 h. The surfaces are then rinsed with six portions of ethanol prior to introduction into the mass spectrometer. For a more detailed description of RSAU surface preparation, see Refs 17 and 18.

An important topic to be considered at this point is the degree of surface damage after ion bombardment and its effects on SID spectra. Ion beam damage to self-assembled monolayer surfaces has been studied in our laboratory[18] and other laboratories,[10a,16] but further work in this area is necessary. The results indicate that ion bombardment with some projectiles can damage the self-assembled monolayer surface; this damage can be monitored by detecting changes in the ion–surface reaction products and/or chemical sputtering products in the SID spectra[18] or by using a separate analysis technique such as IR spectrometry.[10] The damage increases with an increase in the recombination energy of the projectile ion, e.g. argon ions cause much more extensive damage than benzene ions. In spite of detected damage of hydrocarbon surfaces, SID spectra often remain

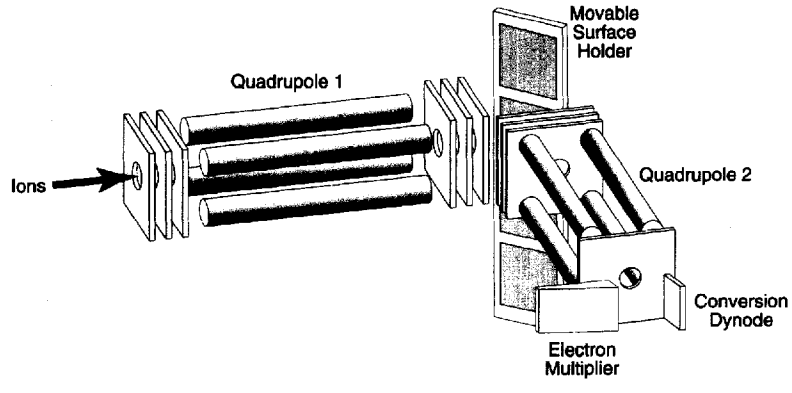

Figure 2. Schematics of an Extrel 4000 u tandem mass spectrometer designed for low-energy ion–surface collisions,[15] with a fourfold surface holder designed to hold multiple surfaces (see text for details).

unchanged after damage,[10a] presumably because the build-up of an adventitious hydrocarbon layer on top of the damaged surface provides a surface with characteristics similar to the original hydrocarbon surface. Changes in the surface are evident from results acquired with fluorinated or deuterated surfaces where hydrocarbon peaks appear in the spectra after surface damage. Damage by even-electron ions such as the protonated peptides described below is less evident. Even over several days of bombardment of a fluorinated surface with a peptide ion beam, the efficiency (relative amount of neutralization) and percentage energy conversion remain constant. Control experiments in which the surface is intentionally damaged with an argon ion beam prior to peptide dissociation experiments indicate that surface damage is detectable, in terms of efficiency and energy conversion, if present.

The lack of damage for many projectiles is remarkable since the assumed ion current densities ($\sim 10^{-9}$ A cm^{-2} for EI) would correspond to destruction of a monolayer in 100 min if the values of damage cross-sections typical of secondary ion mass spectrometric experiments (i.e. 100 $Å^2$) were assumed. Clearly, this is not an appropriate assumption. Surface analysis experiments are planned to address this issue further. In a practical setting, for common organic analytes, the self-assembled monolayer surfaces are robust enough to allow multiple uses such that surfaces generally need to be changed only when the instrument is vented for another purpose (e.g. changing filaments or source types).

SURFACE-INDUCED DISSOCIATION OF SINGLY PROTONATED PEPTIDES: ANALYTICAL ASPECTS

Sequence analysis of peptides by tandem mass spectrometry has developed as an alternative technique to sequencing performed by the well established Edman degradation technique.[32] MS/MS can be performed on small quantities of sample, on mixtures, the presence of modified amino acids can be detected and a free amino terminus is not required for sequencing. With the development of newer ionization techniques such as liquid secondary ion mass spectrometry (LSIMS),[33] electrospray (ESI)[34] and matrix-assisted laser desorption/ionization (MALDI),[35] there is augmented interest in performing structural analyses of biomolecules by tandem mass spectrometry. Currently, most research efforts are centered around activation and fragmentation of peptides by gas-phase collisions with inert gases, specifically low-energy (eV) and high-energy (keV) CID.[32,36–50] Cooks *et al.*[4] were the first to report the fragmentation of peptides by SID on both hybrid (BQ) and modified tandem quadrupole instruments. Since then, several researchers have reported fragmentation of peptides by SID.[21,28,29,31,51–58] Most of these investigations were carried out on commercial tandem instruments to permit SID, but many of the instrument parameters were not optimized and the SID spectra for fragmentation of peptides were obtained at low signal-to-noise ratio and low resolution.

To assess the utility of SID for structure elucidation of peptides, systematic studies were performed by Wysocki and co-workers.[54–58] In one of these investigations, a number of singly protonated peptides varying in size and amino acid sequence and generated by LSIMS were subjected to SID.[54] The results demonstrated extensive and structurally informative fragmentation of precursor peptide ions. The SID fragmentation spectra of singly protonated peptides are dominated by backbone cleavage ions, namely *a*-, *b*- and *y*-type ions, in addition to immonium and internal fragment ions (see Fig. 3). These ion types are analogous to those observed under low-energy gas-phase collisions (CID). In addition to backbone cleavage ions, side-chain specific cleavage ions, namely *d*- and *w*-type ions, normally thought to be characteristic of high-energy (keV) CID, are also observed by low-energy (eV) SID.[54] As described by Biemann and co-workers[48,49] for keV CID, the presence or absence of these side-chain specific fragment ions is dependent on the presence or absence of a basic residue along the peptide backbone. If the basic amino acid residue is located *N*-terminal to the cleavage site, *d*-type ions are formed, and if the basic residue is located *C*-terminal to the cleavage site, *w*-type ions are formed. These ion types (namely *d* and *w*) are formed by charge-remote fragmentation pathways. In contrast, the majority of the fragment ions formed by low-energy (eV) surface or gas-phase collisions are probably formed by charge-directed fragmentation pathways. Although charge-remote fragmentation can be a low-energy process, as illustrated for surfactant ions,[50,59] charge-remote fragmentation tends to be a high-energy process for peptides because of their size and because the fragmentation generally must compete kinetically with lower energy charge-directed pathways. The observation of both charge-directed and charge-remote fragmentation ions by SID is a consequence of high average internal energy deposition in a single-step surface collision compared with the multi-step energy deposition associated with multiple collision low-energy CID. Although the total average internal energy under the multiple collision conditions (low-energy CID) may be higher than that for single collisions with surfaces or high-energy gas-phase collisions, competitive fragmentation processes with lower activation energies (e.g. rearrangements) may dominate low-energy CID spectra, resulting in few or no charge-remote fragmentation processes.

The experimental results discussed thus far are consistent with *ab initio* and MNDO bond order and MNDO energy partitioning calculations performed in our laboratory for model peptides.[54,60,61] The results from the calculations suggest that the amide bond is considerably weakened when an amide nitrogen is protonated (the amide bond order is reduced by about 35% with respect to that of the corresponding neutral), or partially protonated through proton-bridged structures. The cleavage of these weakened amide bonds could lead directly to the energetically preferred formation of *b*-type ions, one of the dominant types of ions observed in low- and high-energy collisional activation (SID or CID) spectra. This is the expected result in spite of the fact that the amide nitrogen is less basic than amide oxygen; charge-directed fragmentation of amide

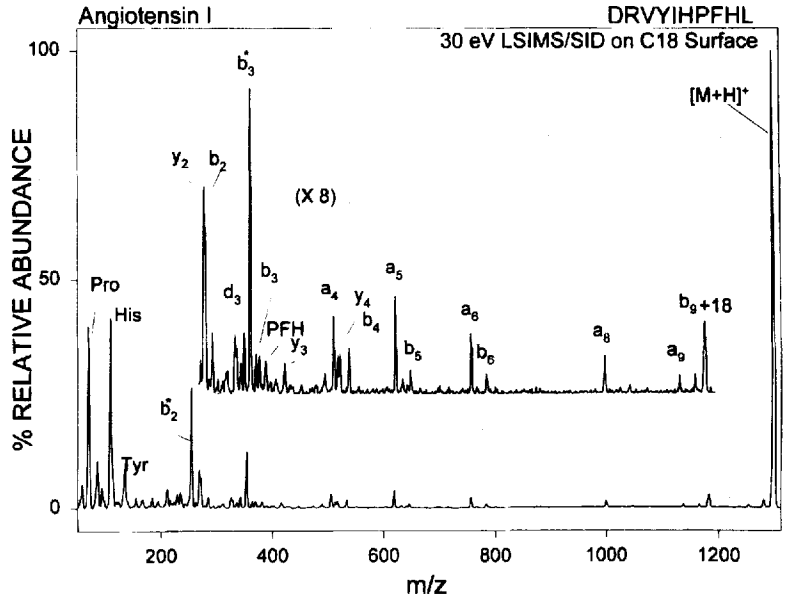

Figure 3. Surface-induced dissociation spectrum of the $[M + H]^+$ ion (*m/z* 1296) of angiotensin I obtained upon 30 eV collisions with a octadecanethiolate monolayer surface. $[M + H]^+$ ions were formed by 6 keV Cs^+ ion bombardment; 50–80 pmol of sample mixed with thioglycerol matrix was applied to the FAB probe tip.

oxygen protonated forms is less likely because the amide bond is strengthened in this protonated form (the amide bond order is increased by about 35–40% with respect to the neutral form).

The calculations show that protonation has a 'localized' effect by changing the bond orders in the immediate vicinity of the protonation site. Thus these calculations are also useful for explaining charge-remote fragmentation processes for the formation of *d*- and *w*-type ions, which are proposed to occur by homolytic cleavage of the C—C backbone bond followed by β–γ bond cleavage of the side-chain.

ENERGETICS AND MECHANISMS FOR FRAGMENTATION OF PROTONATED PEPTIDES

Mobile proton model

Recent results from our laboratory demonstrate the utility of surface-induced dissociation to investigate the energetics and mechanisms of fragmentation of protonated peptides.[56,58] It is difficult to estimate activation energies of peptide fragmentation mainly because (i) there are several competitive fragmentation processes, the activation energies of which are very close to each other, (ii) the internal energy of protonated peptides deposited by the available ionization and activation methods cannot be defined unambigously and (iii) fragmentation rates, or rate constants, for protonated peptides are not known. As far as similar activation energies for competitive processes (e.g. b_i ion formation) are concerned, the introduction of the concept of 'average activation energy' helps in characterizing low-energy (charge-directed) fragmentation processes.[62] The ambiguity in knowing the internal energy supplied can be reduced by applying an experimental method which provides a relatively well defined and narrow internal energy. An important and useful feature of the ESI/SID technique is that this ion formation–ion activation combination provides a relatively narrow internal energy distribution, leading to reliable experimental data for the prediction of relative energetics of peptide fragmentation. Such a capability is also expected to facilitate understanding of fragmentation mechanisms. Several questions, such as the mass effect (the effect of the number of active oscillators or incomplete energy randomization), are still unanswered, and the potential applicability of ESI/SID to answer these questions is currently under investigation. Results from alternative methods of activation, such as thermal decomposition of protonated peptides,[63] and from the application of RRKM theory[62,64] and quantum chemical calculations[65] will also be mentioned below.

In a recent paper[58] from our laboratory, experiments are described which were designed to investigate peptide fragmentation as a function of peptide sequence and size, and the results are represented as fragmentation efficiency curves (plots of percentage fragmentation *vs.* laboratory collision energy; e.g. see Fig. 4). Studies performed in our laboratory demonstrate that different ionization methods (namely LSIMS and ESI) in combination with SID yield similar structural (sequence) information for oligopeptides.[54–58] However, the SID fragmentation efficiency curves obtained by electrospray ionization (ESI/SID) are sharper than those obtained by Cs^+ ion bombardment (LSIMS/SID) [see Fig. 4(a)]. This is the case whether protonated peptides or fixed-charge derivatized peptides are examined, i.e. the difference between LSIMS/SID and ESI/SID cannot be attributed simply to the formation of different populations of protonated forms of a given peptide.[58] This indicates that ions generated by ESI are 'internally colder' than ions generated by LSIMS, and therefore

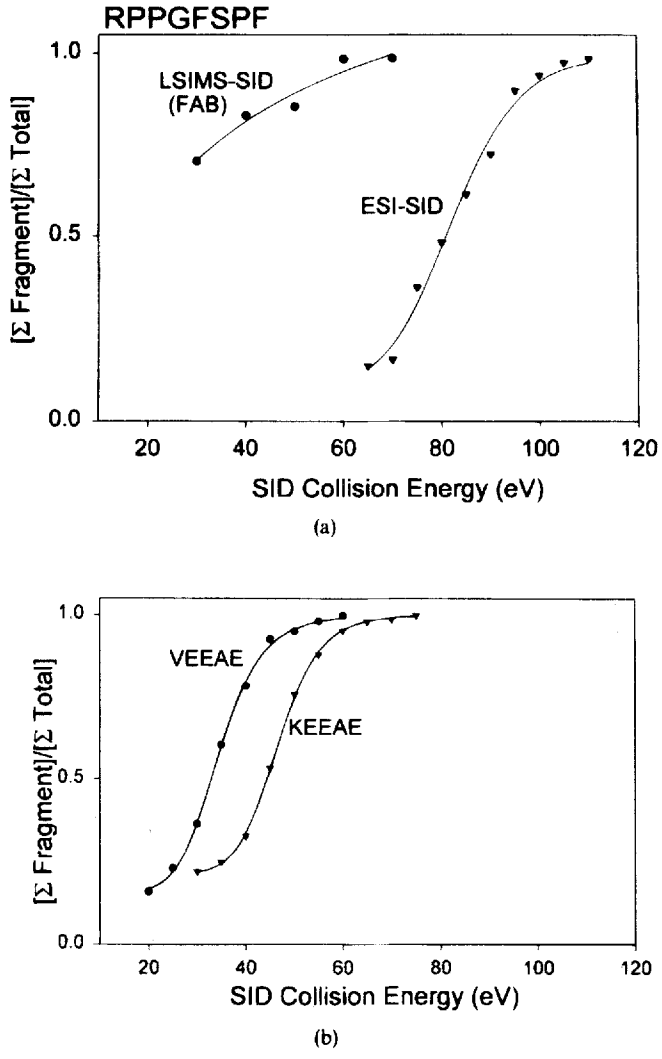

Figure 4. (a) Fragmentation efficiency curves of $[M + H]^+$ ions of des-Arg^9-bradykinin (RPPGFSPF) formed by electrospray (ESI) and liquid secondary ion mass spectrometry (LSIMS) ionization methods. The y-axis represents Σ (fragment ion abundance/Σ (total ion abundance) and the x-axis represents the laboratory collision energy. Adapted from Ref. 56. (b) Fragmentation efficiency curves of $[M + H]^+$ ions of VEEAE and KEEAE formed by ESI. The y-axis represents Σ (fragment ion abundance/Σ (total ion abundance) and the x-axis represents the laboratory collision energy.

LSIMS-generated ions when subjected to SID do not provide sharp fragmentation efficiency curves. In our recent investigations, the relative energetics of peptide dissociation and the dependence of those on peptide size and sequence are demonstrated by the relative positions of the ESI/SID fragmentation efficiency curves. The positions of the ESI/SID fragmentation efficiency curves for various singly charged peptides indicate that peptides containing no basic amino acid residues have lower energy requirements than those containing basic amino acid residues. Within a series of peptides with similar structures, the shifts in the curves can be correlated with gas-phase basicity of the basic amino acid residue present, e.g. peptides containing arginine require the deposition of more energy to fragment than lysine-containing peptides, which in turn require higher energy than peptides without basic amino acid groups (e.g. compare the curve for VEEAE with those for KEEAE [Fig. 4(b)] and RPPGFSPF [Fig. 4(a), ESI/SID curve)]. The relative shifts in the fragmentation efficiency curves correlate to the relative changes in the gas-phase basicity of the peptide that are the result of differences in both their sequence and size (e.g. five different lysine-containing peptides have similar energy requirements for dissociation if a simple degrees of freedom correction is applied to the fragmentation efficiency curve data).[58] This method renders a unique experimental basis to refine and substantiate the 'mobile proton model', a model which describes peptide dissociation under low-energy (eV) collisions (SID or CID) as resulting from charge-directed cleavages initiated by rapid proton transfers along the peptide backbone. This model has been proposed by numerous researchers in various forms and different types of data have been published which are consistent with the hypothesis, although the authors may not have explicitly described their results in terms of the model.

In addition to the results described above, systematic experiments were designed to test the validity of the mobile proton model; these involve comparison of fragmentation efficiency curves of singly and doubly charged ions of a particular peptide, of doubly charged ions of related peptides and of specific chemically modified peptides such as acetylated and fixed-charge derivatized peptides.[58] The relative positions of the fragmentation efficiency curves for singly and doubly charged ions of a particular peptide indicate the plausible initial location of the protons along the backbone and the relative energies required for their mobilization to other sites along the backbone which could lead to fragmenting structures, e.g. curves for singly protonated RPPGFSPF and PPGFSPFR overlap whereas the curves for the doubly charged ions shift to lower energy in a manner consistent with expected basicity of the second most basic site. Fragmentation efficiency curves for acetylated peptides are shifted to lower energies compared with their non-acetylated counterparts, which is in agreement with the fact that acetylation leads to an overall decrease in the gas-phase basicity of the peptide. Similarly, the curves for fixed-charge derivatized peptides are shifted to higher energies compared with their protonated counterparts, which is attributed to charge-remote fragmentation mechanisms operative for fixed-charge derivatized peptides. Certain peptide charge-remote mechanisms are suggested by Biemann and co-workers[47,48] to require homolytic bond cleavage followed by side-chain loss, a two-step process that is expected to be more energetically demanding than simple charge-directed cleavage enhanced by the weakening of the amide bond associated with proton localization, e.g. b ion formation from amide N-protonated form.

Determination of average activation energies

Another application of ESI/SID fragmentation efficiency curves is the determination of average activation energies for the main fragmentation processes of protonated oligopeptides. This is a difficult problem and the ESI/SID curves provide only one approach to tackle

this complex issue. A method applied recently by Vekey *et al.*,[62] is based on using ESI/SID fragmentation efficiency curves and the ratio of kinetic to internal energy conversion in SID to estimate the internal energy of fragmenting ions. Using this internal energy and knowing the average flight time of ions and using RRKM calculations,[64] the average activation energy values can be obtained. This approach has been applied for protonated leucine enkephalin and led to an average activation energy of 36 kcal mol^{-1} (1 kcal = 4.184 kJ) for the lowest energy decompositions.[62] Several other peptides in the mass range of 200–1200 u have also been studied, yielding activation energies in the range of 35–47 kcal mol^{-1}.[62]

Ab initio calculations[65] at the MP2 6–31G*//HF 6–31G* level have also been carried out on fragments of protonated diglycines to estimate the energetics of the formation of *y*, *b* and *a* ions and of NH_3 loss. The predicted values relative to the amide N protonated diglycines are 40.8 and 44.4 kcal mol^{-1} (*y* ion formation), 50.8 kcal mol^{-1} (*b* ion formation), 45.6 kcal mol^{-1} (*a* ion formation from *b* ions by CO loss) and 69.7 kcal mol^{-1} (loss of NH_3). The quantum chemical values are in reasonable agreement with the values predicted by experimental data on thermal dissociation[63] and the present RRKM study just cited.[62]

An alternative way to determine experimentally the average activation energies for fragmentation of protonated oligopeptides is to examine their thermal decomposition. Recently, we have published the rate constants for the unimolecular decomposition of peptide monomer and dimer ions by thermal and surface-induced dissociation.[63] By comparison of the thermal rate constants to those of SID processes, effective SID temperatures (viz. post-collisional temperatures) have been estimated for protonated leucine enkephalin. Thermal decomposition of the protonated leucine enkephalin ion is observed between 600 and 680 K with rate constants of 20–200 s^{-1}, and yields many of the same fragments as SID at 35 eV laboratory collision energy, although with different relative abundances. The thermal decomposition yields the Arrhenius parameters E_a = 38.3 kcal mol^{-1}, log A = 15.7. Based on the distance between the surface and the second quadrupole the SID rate constants were determined to be in the range of 2×10^4 and 40×10^4 s^{-1}, leading to effective temperatures of 710–840 K by extrapolation of the thermal activation parameters. Other experiments comparing thermal and SID fragmentation are in progress in our laboratory. If reliable correlations between thermal decomposition and SID decomposition can be obtained for several oligopeptides, SID could, potentially, be used to estimate 'temperatures' of protonated oligopeptides and, as a consequence, the internal energy of these protonated biomolecules could be determined with an acceptable accuracy.

SURFACE-INDUCED DISSOCIATION OF MULTIPLY PROTONATED PEPTIDES

From the discussion presented in this paper thus far it is clear that SID is an effective activation technique to elucidate primary structures of peptides. In addition, when coupled with an ionization technique such as ESI, the combination (ESI/SID) proves to be a distinctive tool to study the relative energetics and mechanisms of peptide fragmentation. However, an important question still remains to be addressed: can the high internal energy deposition afforded by SID be utilized to fragment large (>2000 u) protonated peptides, which would further enhance the analytical utility of SID as an activation method for MS/MS?

There have been attempts to demonstrate the utility of SID to fragment peptides larger than 2000 u. A collaborative study involving dual-cell FTMS[28] reported the first SID of peptides larger than 2000 u. The SID spectra of atriopeptin III (M_r 2549) and renin substrate tetradecapeptide (M_r 3054) show extensive fragmentation; however, the spectra depict only the low-mass portion of the spectrum (*m/z* 40–800) and no pertinent sequence information over a wide mass range was demonstrated. More recent results of McLafferty and co-workers[29] exhibit the fragmentation of carbonic anhydrase (M_r 29 000) by SID in open cylindrical cell FTMS. The fragmentation yields mainly *b*- and *y*-type ions which are of low abundance and are presented only in the vicinity of the precursor ion.

We report here a systematic study on the fragmentation of multiply protonated peptides in the mass range of 2000–5000 u. Table 1 lists the different bioactive peptides that were selected for analysis based on their size (mass) and amino acid sequence. All the peptide ions were generated by ESI, and several different charge states from the electrosprayed peptide solutions were

Table 1. List of multiply protonated peptides (>2000 u) investigated by surface-induced dissociation

Peptide[a]	M_r	Sequence[b]	Precursor ion charge states investigated
ACTH 18–39	2465	*R*PV*K*VYPNGAEDESAEAFPLEF	$[M+2H]^{2+}$
Melittin (bee venom)	2845	GIGAVL*K*VLTTGLPALISWI*KRKR*QQ-NH_2	$[M+2H]^{2+}$, $[M+3H]^{3+}$
Human β-endorphin	3465	YGGFMTSE*K*SQTPLVTLF*K*NAIILNAY*KK*GE	$[M+3H]^{3+}$
Glucagon (porcine)	3484	HSQGTFTSDYS*K*YLDS*RR*AQDFVQWLMNT	$[M+2H]^{2+}$, $[M+3H]^{3+}$
Bovine insulin B-chain (Ox)	3496	FVNQHLC[SO_3H]GSHLVEALYLVC[SO_3H]GERGFFYTP*K*A	$[M+2H]^{2+}$, $[M+3H]^{3+}$
Human parathyroid hormone 1–34	4118	SVSEIQLMHNLG*K*HLNSME*R*VETL*RKK*LQDVHNF	$[M+4H]^{4+}$
Porcine ACTH 1–39	4568	SYSMEHF*R*WGKPG*KKRR*PV*K*VYPNGAEDELAEAFPLEF	$[M+4H]^{4+}$

[a] All the peptides were purchased from Sigma Chemical and used without further purification.
[b] The peptide sequences are designated by single-letter codes and the basic amino acid groups arginine (R) and lysine (K) are represented in italics.

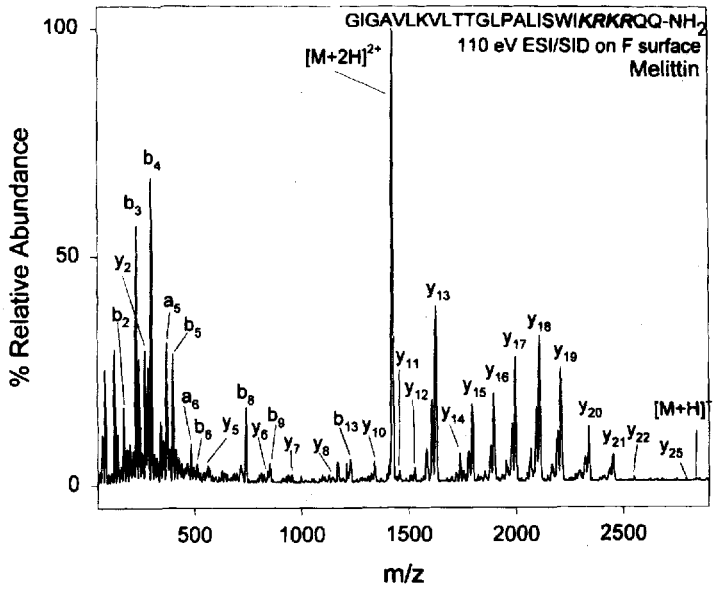

Figure 5. Surface-induced dissociation spectrum of doubly-protonated Melittin (GIGAVLKVLTTGLPALISWI*KRKR*QQ-NH_2) obtained upon a 110 eV collision with a 2-(perfluorooctyl) ethanethiolate monolayer surface.

mass-selected and made to collide with a fluorinated alkanethiolate monolayer surface to undergo fragmentation. Several SID spectra will be presented here to illustrate (i) the influence of location and concentration of basic amino acid groups along the peptide backbone on the type of fragment ions observed and (ii) the influence of mass-selected precursor ion charge state on the charge state of the fragment ions observed. Wherever possible the SID spectra are compared with published low-energy (EV)[34d,36] and high-energy (keV)[66] CID spectra.

The SID spectra of all the multiply protonated peptides (see Figs 5–9) yield mainly backbone cleavage ions, i.e. *a*-, *b*- and *y*-type ions. Except in the case of bovine insulin B-chain (oxidized), all the other peptides investigated here have a concentration of basic amino acid groups, namely Arg (R) and Lys (K), somewhere along the peptide backbone (see Table 1). All the SID spectra show that precursor ions with n charges lose a proton upon collision with the surface to yield an $n-1$ charged species of the intact peptide, i.e. $[M+4H]^{4+}$ yields $[M+3H]^{3+}$. This information can also be useful and can be exploited to confirm the molecular masses of unknown peptides. In the case of melittin (from bee venom), a KRKR segment is close to the *C*-terminus of the peptide and the SID spectra of both the doubly and triply charged precursor of melittin are dominated by *y* ions (see Fig. 5 and Ref. 63). The SID spectrum of doubly charged melittin yields a singly-charged *y* ion series from y_2 to y_{25} with the exception of y_3, y_4, y_{23}

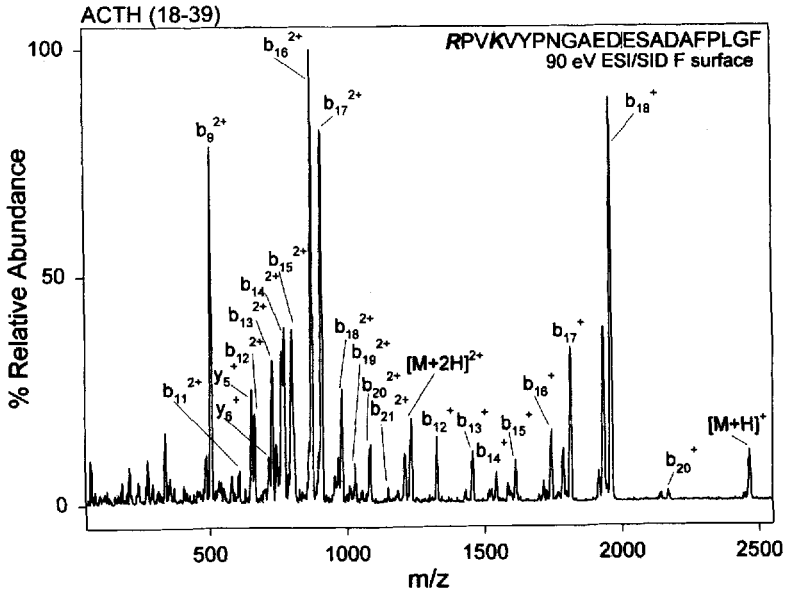

Figure 6. Surface-induced dissociation spectrum of doubly charged ACTH (18–39) (*R*PV*K*VYPNGAEDESADAFPLGF) obtained upon a 90 eV collision with a 2-(perfluorooctyl) ethanethiolate monolayer surface.

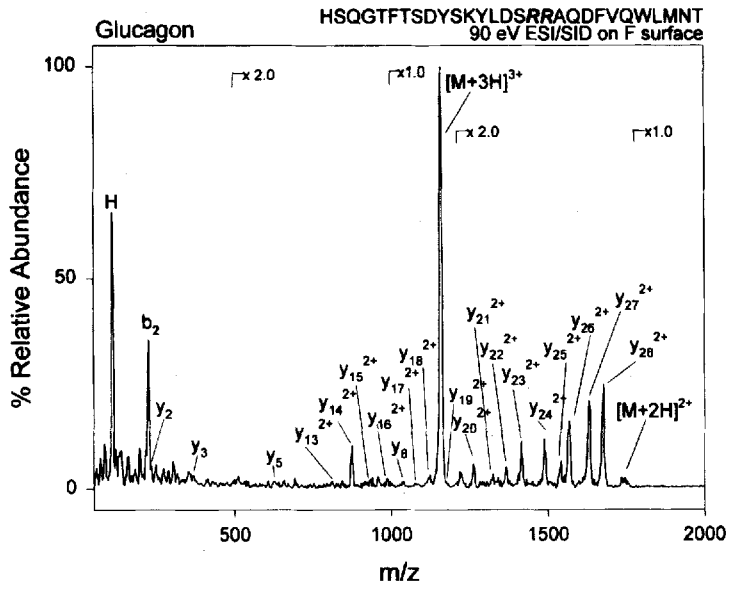

Figure 7. Surface-induced dissociation spectrum of triply charged glucagon obtained (HSQGTFTSDYS*K*YLDS*RR*AQDFVQWLMNT) upon a 90 eV collision with a 2-(perfluorooctyl) ethanethiolate monolayer surface.

and y_{24}. In addition, a series of satellite peaks are observed for the y ions which are due to sequential losses of 17 u and 28 u from a given y ion (melittin has a carboxy-terminal amide which could explain the above losses). With the exception of two residues, a complete primary sequence for melittin can be obtained from this spectrum. Note, when our SID spectra were submitted for primary sequence analysis, Sequest (written by Yates and coworkers[66]) yielded excellent correlation (99%) to the melittin sequence in the proteins database. Recently published SID spectra of melittin by McLafferty and co-workers ($[M + 4H]^{4+}$ selected) also show predominantly y-type ions, however, the sequence information is not complete and unambiguous.[29] In contrast, in the case of adrenocorticotropic hormone (ACTH clip 18–39), collision of the doubly charged precursor ions with a fluorinated surface yields predominantly singly and doubly charged b ion series, which is in agreement with CID results for peptides with arginine and/or lysine at the N-terminus of the peptide (see Fig. 6). In the cases of glucagon (porcine) and porcine ACTH 1–39 (see Table 1; the sequences indicate the presence of basic amino acid groups in the middle of the peptide backbone), the SID spectra are dominated by a y ion series (Fig. 7) and a b ion series (Fig. 8), respectively. For ACTH 1–39 the 100 eV SID spectrum ($[M + 4H]^{4+}$) is similar to those acquired by CID of $[M + 5H]^{5+}$, $[M + 6H]^{6+}$ and

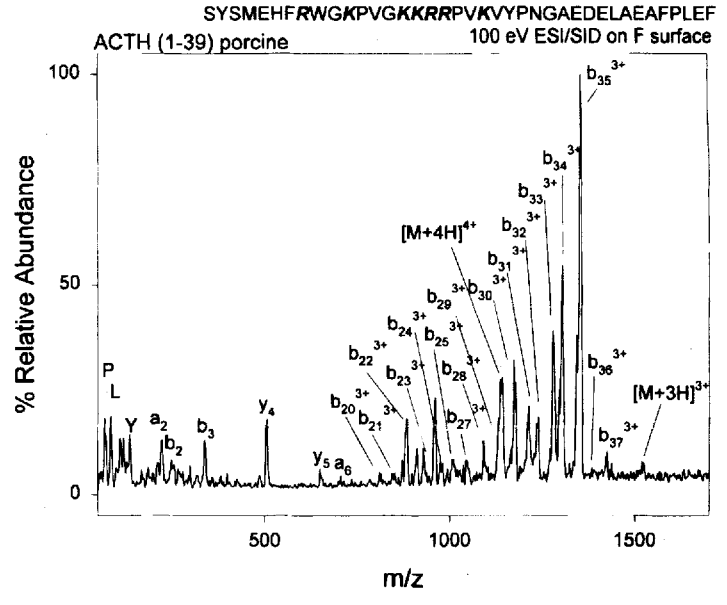

Figure 8. Surface-induced dissociation spectrum of quadruply charged porcine ACTH 1–39 (SYSMEHF*R*WGKPG*KKRR*PV*K*VYPNGAEDELAFPLEF) obtained upon a 100 eV collision with a 2-(perfluorooctyl) ethanethiolate monolayer surface.

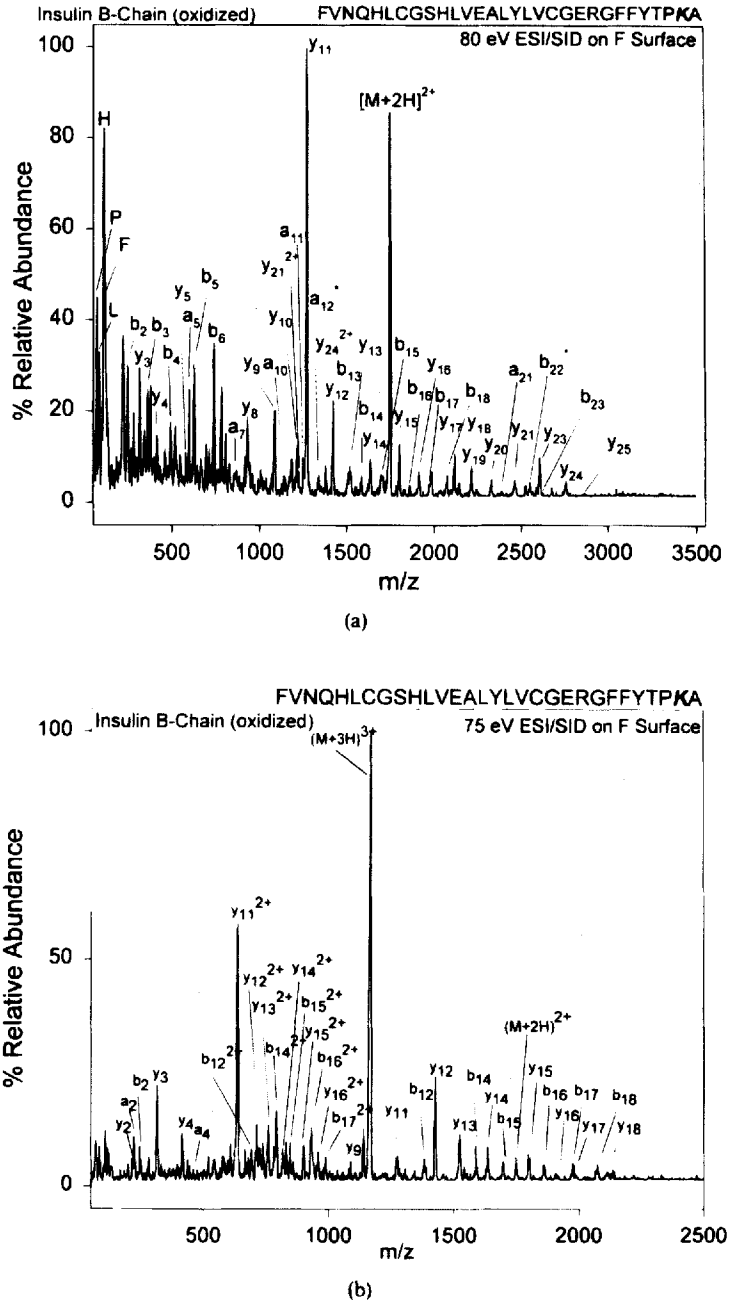

Figure 9. Surface-induced dissociation spectra of (a) doubly charged and (b) triply charged insulin B-chain (FVNQHLCGSHLVEALYLVCGERGERGFFYTPKA) obtained upon an 80 eV collision with a 2-(perfluorooctyl) ethanethiolate monolayer surface.

$[M + 7H]^{7+}$ at 780 eV collision energy.[34d] In the case of bovine insulin B-chain (oxidized), where there is a singly basic amino acid group (lysine) close to the *C*-terminus, both *b*- and *y*-type fragment ions are observed in the case of both doubly and triply charged precursors (see Fig. 9). Peptides similar to those in Table 1 have also been investigated by high-energy gas-phase collisions by Fenselau and co-workers.[67] The high-energy (keV) CID spectra yield fragment ions over a small mass range in the vicinity of the precursor ion selected. In addition to backbone cleavage ions (*a*-, *b*- and *y*-type ions), side-shain cleavage *d*-, *w*- and *v*-type ions are also observed. However, the spectra do not provide extended series of sequence ions of the same type, making it difficult to obtain unambiguous sequence information (e.g. compare the SID spectra of melittin[63] (see also Fig. 5) with the keV CID spectra[67]).

In synopsis, although much work remains, SID demonstrates promise as an activation method to obtain structurally relevant (primary sequence) information of large (>2000 u) bioactive oligopeptides. For oligopeptides greater than 5000 u, additional experiments are required to demonstrate the utility of SID to obtain both structural and mechanistic information. However, the recent results by McLafferty and co-workers[29] demonstrating fragmentation of carbonic anhydrase (M_r

29 000) indicates a promising start for extensive applicability of SID as an activation technique for MS/MS.

CONCLUSIONS

An important characteristic of SID is that it deposits, in the selected projectile ions, significant amounts of internal energy in a controllable manner. For protonated peptides generated by LSIMS or ESI, high-quality dissociation spectra are produced by SID. ESI/SID results obtained by exploiting the controllable energy deposition are providing new information on peptide fragmentation energetics and mechanisms, in addition to determining or confirming sites of proton localization in singly and multiply protonated peptides. In addition, ESI/SID experimental data obtained from fragmentation efficiency curves, in combination with experimental data from thermal decomposition studies, may provide a basis for the calculation of average activation energies of low-energy fragmentation processes for peptides.

So far, SID has been used in a relatively small number of laboratories and SID of biomolecules has been investigated in only a subset of these laboratories. The recent promising data acquired for protonated peptides by SID should encourage instrument companies to incorporate SID into commercial tandem mass spectrometers. We are confident that commercially available SID instruments will open new dimensions in structural investigations.

Acknowledgements

This work was financially supported by a grant from the National Institute of Health (GM 51387). The authors thank Dr A. L. McCormack and Dr J. R. Yates for analyzing SID spectra by Sequest.

REFERENCES

1. K. L. Busch, G. L. Glish and S. A. McLuckey, *Mass Spectrometry/Mass Spectrometry: Techniques and Applications of Tandem Mass Spectrometry*. VCH, New York (1988).
2. E. de Hoffmann, *J. Mass Spectrom.* **31**, 129 (1996).
3. (a) R. G. Cooks, T. Ast and J. H. Beynon, *Int. J. Mass Spectrom. Ion Phys.* **16**, 348 (1975); (b) MD. A. Mabud, M. J. Dekrey and R. G. Cooks, *Int. J. Mass Spectrom. Ion Processes* **67**, 285 (1985).
4. R. G. Cooks, J. W. Amy, M. E. Bier, J. C. Schwartz and K. L. Schey, *Adv. Mass Spectrom*, **11**, 33 (1989).
5. R. G. Cooks, T. Ast and M. A. Mabud, *Int. J. Mass Spectrom. Ion Processes* **100**, 209 (1990).
6. M. J. Dekrey, H. I. Kenttämaa, V. H. Wysocki and R. G. Cooks, *Org Mass Spectrom.* **21**, 193 (1986).
7. M. Morris, D. E. Riederer, Jr, R. G. Cooks, T. Ast and C. E. D. Chidsey, *Int. J. Mass Spectrom. Ion Processes* **122**, 181 (1992).
8. S. A. Miller, D. E. Riederer, Jr, R. G. Cooks, W. R. Cho, H. W. Lee and H. Kang, *J. Phys. Chem.* **98**, 245 (1994).
9. T. Pradeep, S. A. Miller and R. G. Cooks, *J. Am. Soc. Mass Spectrom.* **4**, 769 (1993).
10. (a) J. A. Burroughs and L. Hanley, *Anal. Chem.* **66**, 3644 (1994); (b) J. A. Burroughs, S. B. Wainhaus and L. Hanley, *J. Phys. Chem.* **98**, 10913 (1994).
11. T. Zhong and D. P. Ridge, in *Proceedings of 41st ASMS Conference on Mass Spectrometry and Allied Topics, San Francisco, CA, 1993*, p. 177.
12. (a) R. D. Beck, P. M. St. John, M. L. Homer and R. L. Whetten, *Science* **253**, 879 (1991); (b) P. M. St. John, R. D. Beck, and R. L. Whetten, *Phys. Rev. Lett.* **69**, 1467 (1992); (c) P. M. St. John and R. L. Whetten, *Chem. Phys. Lett.* **196**, 330 (1992).
13. V. H. Wysocki, J. L. Jones and J.-M. Ding, *J. Am. Chem. Soc.* **113**, 8967 (1991).
14. K. Vékey, Á. Somogyi and V. H. Wysocki, *J. Mass Spectrom*, **30**, 212 (1995).
15. V. J. Angelico, T. E. Kane, Á. Somogyi and V. H. Wysocki, in preparation.
16. R. G. Cooks, T. Ast, T. Pradeep and V. H. Wysocki, *Acc. Chem. Res.* **27**, 316 (1994).
17. Á. Somogyi, T. E. Kane, M.-J. Ding and V. H. Wysocki, *J. Am. Chem. Soc.* **113**, 5275 (1993).
18. T. E. Kane, Á. Somogyi and V. H. Wysocki, *Org. Mass Spectrom.* **28**, 1665 (1993).
19. J. H. Callahan, Á. Somogyi and V. H. Wysocki, *Rapid Commun. Mass Spectrom.* **7**, 693 (1993).
20. M. J. Hayward, F. D. S. Park, L. M. Manzella and S. I. Bernasek, *Int. J. Mass Spectrom. Ion Processes* **148**, 25 (1995).
21. (a) K. L. Schey, D. A. Durkin and K. R. Thornburg, *J. Am. Soc. Mass Spectrom*, **6**, 257 (1995); (b) D. Despeyroux, A. Wright and K. Jennings, *Int. J. Mass Spectrom. Ion Processes* **126**, 95 (1993); (c) A. D. Wright, D. Despeyroux, K. R. Jennings, S. Evans and A. Riddoch, *Org. Mass Spectrom.* **27**, 525 (1992).
22. (a) M. E. Bier, J. W. Amy, R. G. Cooks, J. E. P. Syka, P. Ceja and G. Stafford, *Int. J. Mass Spectrom. Ion Processes* **77**, 31 (1987); (b) M. E. Bier, J. C. Schwartz, K. L. Schey and R. G. Cooks, *Int. J. Mass Spectrom. Ion Processes* **103**, 1 (1990).
23. V. H. Wysocki, J.-M. Ding, J. L. Jones, J. H. Callahan and F. L. King, *J. Am. Soc. Mass Spectrom.* **3**, 27 (1992).
24. A. Duhr, J. Stadlmann, P. Stracke and W. Wollnik, in *Proceedings of 43rd ASMS Conference on Mass Spectrometry and Allied Topics, Atlanta, GA, 1995*, p. 139.
25. K. L. Schey, R. G. Cooks, A. Kraft, R. Grix and H. Wollnik, *Int. J. Mass Spectrom. Ion Processes* **91**, 1 (1989).
26. E. R. Williams, L. Fang and R. N. Zare, *Int. J. Mass Spectrom. Ion Processes* **123**, 233 (1993).
27. (a) C. F. Ijames and C. L. Wilkins, *Anal. Chem.* **62**, 1295 (1990); (b) J. A. Castoro, L. M. Nuwaysir, C. F. Ijames and C. L. Wilkins, *Anal. Chem.* **64**, 2238 (1992).
28. E. R. Williams, K. D. Henry, F. W. McLafferty, J. Schabanowitz and D. F. Hunt, *J. Am. Soc. Mass Spectrom.* **1**, 413 (1990).
29. R. A. Chorush, D. P. Little, S. C. Beu, T. D. Wood and F. W. McLafferty, *Anal. Chem.* **67**, 1042 (1995).
30. S. A. Lammert and R. G. Cooks, *J. Am. Soc. Mass Spectrom.* **2**, 487 (1991).
31. W. Aberth, *Anal. Chem.* **62**, 609 (1990).
32. (a) S. A. Carr, M. E. Hemling, M. F. Bean and G. D. Roberts, *Anal. Chem.* **63**, 2802 (1991); (b) D. F. Hunt, J. R. Yates, III, J. Shabanowitz, S. Winston and C. R. Hauer, *Proc. Natl. Acad. Sci. USA* **86**, 6233 (1986); (c) K. Biemann and H. A. Scoble, *Science* **237**, 992 (1987).
33. C. Fenselau and R. J. Cotter, *Chem. Rev.* **87**, 501 (1987).
34. (a) M. Dole, L. L. Mack, R. L. Hines, R. C. Mobley, L. D. Ferguson and M. B. Alice, *J. Chem. Phys.* **49**, 2240 (1968); (b) J. B. Fenn, J. B. M. Mann, C. K. Meng, S. F. Wong and C. M. Whitehouse, *Science* **246**, 64 (1989); (c) M. Mann, C. K. Meng and J. B. Fenn, *Anal. Chem.* **61**, 1702 (1989); (d) R. D. Smith, J. A. Loo, C. G. Edmonds, C. J. Barinaga and H. R. Udseth, *Anal. Chem.* **62**, 882 (1990).
35. (a) M. Karas, U. Bachman and F. Hillenkamp, *Int. J. Mass Spectrom. Ion Processes* **78**, 53 (1987); (b) F. Hillenkamp, M. Karas, M. R. C. Beavis and B. T. Chait, *Anal. Chem.* **63**, 1193A (1991).
36. R. D. Smith, J. A. Loo, C. J. Barinaga, C. G. Edmonds and H. R. Udseth, *J. Am. Soc. Mass Spectrom*, **1**, 53 (1990).

37. K. Biemann, *Methods Enzymol.* **193**, 351, 455 (1990).
38. R. A. Yost and R. K. Boyd, *Methods Enzymol.* **193**, 154 (1990).
39. M. L. Gross, *Methods Enzymol.* **193**, 131 (1990).
40. K. B. Tomer, *Mass Spectrom. Rev.* **8**, 445, 483 (1989).
41. K. Biemann, *Biomed. Environ. Mass Spectrom.* **16**, 99 (1988).
42. (a) D. F. Hunt, R. A. Henderson, J. Shabanowitz, K. Sakaguchi, H. Michel, N. Sevilir, A. L. Cox, E. Appella and V. H. Engelhard, *Science* **255**, 1261 (1992); (b) D. F. Hunt, H. Michel, T. A. Dickinson, J. Shabanowitz, A. L. Cox, K. Sakaguchi, E. Appella, H. M. Grey and A. Sette, *Science* **256**, 1817 (1992).
43. M. F. Bean, S. A. Carr, G. C. Thorne, M. H. Reilley and S. J. Gaskell, *Anal. Chem.* **63**, 1473 (1991).
44. A. J. Alexander, P. Thibault, R. K. Boyd, J. M. Curtis and K. L. Rinehart, *Int. J. Mass Spectrom. Ion Processes* **98**, 107 (1990).
45. L. Poulter and L. C. E. Taylor, *Int. J. Mass Spectrom. Ion Processes* **91**, 183 (1989).
46. K. D. Ballard and S. J. Gaskell, *Int. J. Mass Spectrom. Ion Processes* **111**, 173 (1991).
47. K. Biemann and S. A. Martin, *Mass Spectrom. Rev.* **6**, 1 (1987).
48. R. S. Johnson, S. A. Martin, K. Biemann, J. T. Stults and J. T. Watson, *Anal. Chem.* **59**, 2621 (1987).
49. R. S. Johnson, S. A. Martin and K. Biemann, *Int. J. Mass Spectrom. Ion Processes* **86**, 137 (1988).
50. A. J. Alexander, P. Thibault and R. K. Boyd, *Rapid Commun. Mass Spectrom.* **3**, 30 (1989).
51. A. R. Dongre, M. J. Hayward and V. H. Wysocki, in *Proceedings of 42nd ASMS Conference on Mass Spectrom and Allied Topics, 1995.*
52. R. B. Cole, S. LeMeillour and J.-C. Tabet, *Anal. Chem.* **64**, 365 (1992).
53. A. L. McCormack, J. L. Jones and V. H. Wysocki, *J. Am. Soc. Mass Spectrom.* **3**, 859 (1992).
54. A. L. McCormack, Á. Somogyi, A. R. Dongré and V. H. Wysocki, *Anal. Chem.* **65**, 2859 (1993).
55. V. H. Wysocki, J. L. Jones, A. R. Dongré, Á. Somogyi and A. L. McCormack, in *Biological Mass Spectrometry: Present and Future*, Chapt. 2.14, pp. 249–254. Wiley, New York (1994).
56. J. L. Jones, A. R. Dongré, Á. Somogyi and V. H. Wysocki, *J. Am. Chem. Soc.* **116**, 8368 (1994).
57. (a) V. H. Wysocki and A. R. Dongré, in *Large Ions: Their Vaporization, Detection and Structural Analysis*, edited by T. Baer. Wiley, New York, in press; (b) A. R. Dongré, Á. Somogyi and V. H. Wysocki, in *Proceedings of 43rd ASMS Conference on Mass Spectrometry and Allied Topics, Atlanta, GA, 1995*, p. 353.
58. A. R. Dongré, J. L. Jones, Á. Somogyi and V. H. Wysocki, in press.
59. (a) V. H. Wysocki, M. E. Bier and R. G. Cooks, *Org. Mass Spectrom.* **23**, 627 (1988); (b) V. H. Wysocki and M. M. Ross, *Int. J. Mass Spectrom. Ion Processes* **104**, 179 (1991).
60. Á. Somogyi, V. H. Wysocki and I. Mayer, *J. Am. Soc. Mass Spectrom.* **5**, 704 (1994).
61. Á. Somogyi, V. H. Wysocki and I. Mayer, submitted for publication.
62. The term 'average activation energy' has been introduced in a recent paper by K. Vékey, Á. Somogyi and V. H. Wysocki, submitted for publication. The average activation energy determined here will be an average value of those processes, which give abundant ions at the internal energy studies, i.e. the energy sufficient to induce fragmentation of ~50% of the ions (at the inflection point of the fragmentation efficiency curves).
63. M. Meot-Ner (Mautner), A. R. Dongré, Á. Somogyi and V. H. Wysocki, *Rapid Commun. Mass Spectrom.* **9**, 829 (1995).
64. P. J. Derrick, P. M. Loyd and J. R. Christie, *Adv. Mass Spectrom.* **13**, 000 (1995).
65. Á. Somogyi and V. H. Wysocki, unpublished results.
66. J. K. Eng, A. L. McCormack and J. R. Yates III, *J. Am. Soc. Mass Spectrom.* **5**, 976 (1994).
67. D. Fabris, M. Kelly, C. Murphy, Z. Wu and C. Fenselau, *J. Am. Soc. Mass Spectrom.* **4**, 652 (1993).